*AAPS PharmSciTech, Vol. 11, No. 1, March 2010 (© 2010)*
DOI: 10.1208/s12249-010-9382-3

*Research Article*

# Freeze Thaw: A Simple Approach for Prediction of Optimal Cryoprotectant for Freeze Drying

**Praveen V. Date,[1] Abdul Samad,[2] and Padma V. Devarajan[1,3]**

*Received 28 July 2009; accepted 12 January 2010; published online 25 February 2010*

***Abstract.*** The present study evaluates freeze thaw as a simple approach for screening the most appropriate cryoprotectant. Freeze–thaw study is based on the principle that an excipient, which protects nanoparticles during the first step of freezing, is likely to be an effective cryoprotectant. Nanoparticles of rifampicin with high entrapment efficiency were prepared by the emulsion-solvent diffusion method using dioctyl sodium sulfosuccinate (AOT) as complexing agent and Gantrez AN-119 as polymer. Freeze–thaw study was carried out using trehalose and fructose as cryoprotectants. The concentration of cryoprotectant, concentration of nanoparticles in the dispersion, and the freezing temperature were varied during the freeze–thaw study. Cryoprotection increased with increase in cryoprotectant concentration. Further, trehalose was superior to fructose at equivalent concentrations and moreover permitted use of more concentrated nanosuspensions for freeze drying. Freezing temperature did not influence the freeze–thaw study. Freeze-dried nanoparticles revealed good redispersibility with a size increase that correlated well with the freeze–thaw study at 20% *w/v* trehalose and fructose. Transmission electron microscopy revealed round particles with a size ~400 nm, which correlated with photon correlation spectroscopic measurements. Differential scanning calorimetry and X-ray diffraction suggested amorphization of rifampicin. Fourier transfer infrared spectroscopy could not confirm interaction of drug with AOT. Nanoparticles exhibited sustained release of rifampicin, which followed diffusion kinetics. Nanoparticles of rifampicin were found to be stable for 12 months. The good correlation between freeze thaw and freeze drying suggests freeze–thaw study as a simple and quick approach for screening optimal cryoprotectant for freeze drying.

**KEY WORDS:** cryoprotectants; freeze drying; freeze thaw; nanoparticles; rifampicin.

## INTRODUCTION

The advantages shown by nanoparticles in the pharmaceutical field have been previously reported in many papers (1,2). Nanocarriers can provide targeted (cellular/tissue) delivery of drugs, to improve oral bioavailability, to sustain drug effect in target tissue, to solubilize drugs for intravascular delivery, and to improve the stability of therapeutic agents against enzymatic degradation (3–10).

Nevertheless, the major obstacle that limits the use of the nanoparticles is their physical instability (aggregation/particle fusion) and/or to the chemical instability (hydrolysis of polymer materials forming the nanoparticles, drug leakage of nanoparticles, and chemical reactivity of medicine during the storage), which are frequently noticed when these nanoparticle are stored as aqueous suspensions for extended periods (11–14). Freeze drying, also known as lyophilization, is an industrial process which consists of removing water from a frozen sample by sublimation and desorption under vacuum. Hence, freeze drying is the recommended method to stabilize and facilitate the handling of colloidal systems, which if stored as suspensions would exhibit instability in a short time. Freeze drying of liposomes (15–17) and solid lipid nanoparticles has been widely discussed (18–21). In contrast, there is limited data on freeze drying of polymeric nanoparticles (22–26). Freeze drying generates various stresses both during freezing and drying (7) and is schematically depicted in Fig. 1. These stresses often result in significant increase in particle size due to agglomeration. Freezing however is the more aggressive step. Cryoprotectants/lyoprotectants are known to provide protection against such stresses (18,24,27). Optimization of both type and concentration of cryoprotectant/s may necessitate studies on a large number of formulations. This can be very tedious and time consuming. Moreover freeze drying is an expensive process.

Freeze–thaw study is short and quick as compared to freeze drying and hence can be used as a pre-test for screening of type and concentration of cryoprotectants used in freeze drying. Freeze–thaw study is based on the principle that if an excipient cannot protect the nanoparticles during the first step of freezing, during lyophilization, it is not likely to be an effective cryoprotectant (18). The aim of the present study is the preparation of polymeric nanoparticles of

[1] Department of Pharmaceutical Sciences and Technology (Deemed University), Institute of Chemical Technology, N.P. Marg, Matunga (E), Mumbai 400019, Maharastra, India.
[2] Bombay Veterinary College, Parel, Mumbai 400012, India.
[3] To whom correspondence should be addressed. (e-mail: pvdevarajan@gmail.com)

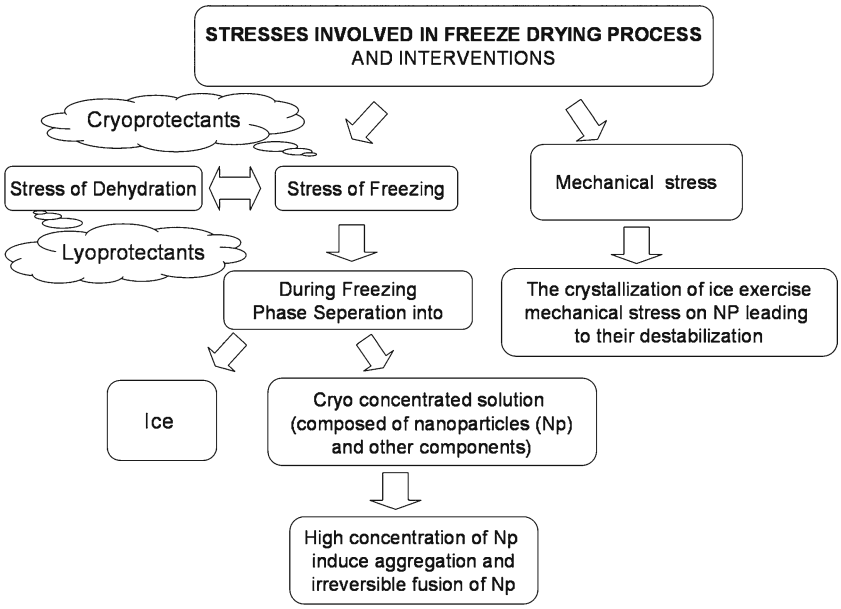


**Fig. 1.** Stresses involved in freeze drying and the interventions to prevent against such stresses

rifampicin. The specific objective of this paper is to evaluate the freeze–thaw approach for optimizing cryoprotectants during freeze drying.

Rifampicin, an antitubercular drug, has been selected for preparation of nanoparticles that could be targeted to alveolar macrophages. Trehalose has been selected as it is considered the best cryoprotective agent among the available carbohydrates (7,18,23,28). It has many advantages in comparison with the other sugars as less hygroscopicity, an absence of internal hydrogen bonds, which allows more flexible formation of hydrogen bonds with nanoparticles during freeze drying, very low chemical reactivity, and finally, higher glass transition temperature, in fact highest glass transition temperatures ($T_g$) of all saccharides commonly used (TREHA™, trehalose by Hayashibara, Japan). It has been proved that trehalose is more effective for stabilizing both compritol (glycerol behenate) and dynasan 112 (glycerol trilaurate) solid lipid nanoparticles during freeze drying at concentration at 15% (18). Fructose has been selected, as an earlier study in our laboratory, has revealed fructose to be a better cryoprotectant for freeze drying of solid lipid nanoparticles (unpublished data).

## MATERIALS AND METHODS

### Materials

Rifampicin (RFM), Gantrez® AN 119 (ISP) (poly methylvinylether maleic anhydride copolymer), poly vinyl alcohol (PVA) (mol wt.25,000), and trehalose 100 (Hayashibara Co. Ltd., Japan) were kindly gifted by Maneesh Pharma (Mumbai, India), Anshul Agencies (Mumbai, India), Colorcon Asia Pvt ltd, and Gangwal Chemicals Pvt. Ltd. (Mumbai, India), respectively. Methyl ethyl ketone AR, Methanol AR, D(–) fructose AR, and dioctyl sodium sulphosuccinate (Aerosol OT, AOT) AR, disodium hydrogen phosphate AR, and sodium chloride AR were purchased from s. d. fine-chem limited (Mumbai, India). Ethyl alcohol AR (99.9% pure) was purchased from Changshu Yangyuan Chemical (China). Magnesium acetate tetrahydrate pure (assay—98–102%), potassium dihydrogen phosphate GR, and hydrochloric acid about 35% pure were purchased from Merck.

### Preparation of Nanoparticles of Rifampicin

Polymeric nanoparticles of rifampicin (RFMNp) were prepared by emulsion-solvent diffusion using Gantrez AN 119 as polymer and methyl ethyl ketone (MEK) as the organic phase. AOT was used as an ionic complexing agent. RFM (20 mg) and Gantrez AN-119 (20–100 mg) were dissolved in a mixture of MEK (4.5 ml) and ethanol (0.5 ml) and added dropwise to an aqueous phase (5 ml) containing AOT (10–30 mg) and PVA (10–30 mg) with continuous stirring on magnetic stirrer, to form a primary emulsion (MEK being partially miscible with water). The primary emulsion was diluted with water (12 ml), followed by addition of magnesium acetate solution as crosslinking agent (3 ml; 5% *w*/*v* solution). The nanoparticle dispersion was kept under stirring for approximately 2 h at 28±2°C till complete evaporation of organic solvent. The nanoparticle dispersion was centrifuged at 15,000 rpm for 30 min, the pellet washed repeatedly with water, and the supernatants were pooled.

### Entrapment Efficiency

The concentration of RFM in the supernatant was determined by UV–Visible spectrophotometry at 475 nm. Entrapment efficiency was using Eq. 1:

$$\text{Entrapment efficiency}\ (\%) = \left(RFM_{initial} - RFM_{supernatant}\right)/RFM_{initial} \times 100 \quad (1)$$

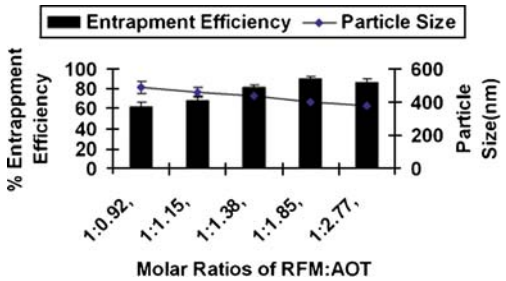


**Fig. 2.** Effect of RFM/AOT ratio on entrapment efficiency and particle size of rifampicin nanoparticles

### Particle Size

Particle size was determined by photon correlation spectroscopy using N4 plus submicron particle size analyzer (Beckman Coulter, USA). The analysis was performed at a scattering angle of 90° at a temperature of 25°C. All the nanoparticulate dispersions were sonicated using ultrasonic probe system (DP120, Dakshin, Mumbai, India) for 5 min with 10-s pulse at 200 V over an ice bath. Dispersions were then appropriately diluted with filtered water (0.2 μm filter, Millipore India Pvt. Ltd.) to obtain $5\times10^4$ to $1\times10^6$ counts per second. Each sample was analyzed in triplicate, and average particle size and polydispersity index (PI) were measured.

### Freeze–Thaw Study

Freeze–thaw study was carried out by subjecting nanoparticle dispersion to freezing for 12 h in a deep freezer (Eclipse 400, RS Biotech, UK) followed by thawing at 28°C. The particle size and PI before freezing and after thawing were determined by PCS.

*Effect of type and concentration of cryoprotectant.* Aliquots of RFMNp having concentration of 32 mg/ml were taken in vials, and two cryoprotectants namely trehalose and fructose were added to obtain cryoprotectant concentrations of 5%, 10%, 15%, and 20% *w/v*.

*Effect of nanoparticle concentration.* The effect of concentration of nanoparticles on freeze–thaw study was assessed, by subjecting different concentrations of nanoparticles, i.e., 8, 16, 32, and 64 mg/ml to the freeze–thaw study using trehalose and fructose as cryoprotectants at 20% *w/v* concentration. All the samples were sonicated in bath sonicator for 1 min prior to freezing at −40°C. Samples were allowed to thaw at room temperature (28°C).

*Effect of freezing temperature.* The effect of freezing temperature on freeze–thaw study was also assessed by carrying out the freeze–thaw study of nanoparticles having concentrations of 8, 16, 32, and 64 mg/ml using 20% *w/v* trehalose and 20% *w/v* fructose as cryoprotectant at −40°C and −70°C.

### Freeze Drying of RFMNp

Freeze drying of two RFMNp batches, one showing minimal change in particle size containing 20% *w/v* trehalose as cryoprotectant and the other showing significant increase in particle size containing 20% *w/v* fructose as cryoprotectant, were carried out using Labconco freeze-drying system (FreeZone 4.5, USA). Samples of 5 ml of dispersion with concentrations of 32 mg/ml of nanoparticles, were dispensed in 100-ml glass vessels, frozen at −40°C for 12 h, and then subjected to freeze drying. Sublimation lasted for 36 h at a vacuum pressure of $54\times10^{-3}$ bar without heating, with the condenser surface temperature maintained at −54°C. Lyophilized samples were collected under anhydrous conditions and stored in a dessicator until re-hydrated. Re-hydration of lyophilized RFMNp was carried with 0.2 μm filtered water by simple manual shaking. Particle size and PI of the re-hydrated samples were determined by PCS to assess the cryoprotection provided by the cryoprotectant. Freeze-dried nanoparticles were evaluated for the following points discussed below.

### *In Vitro* Drug Release

Drug-release studies were performed by the dialysis method (29). Nanoparticles (equivalent to 10 mg drug) were loaded into a pre-treated dialysis bag (Sigma, molecular weight cut-off 12–14 kDa) and introduced into the basket of USP apparatus-I. Phosphate-buffered saline (900 ml) containing 1% *w/v* ascorbic acid and 0.05% *w/v* sodium azide, at a pH of 7.2, was used as the dissolution medium (30). Aliquots (5 ml) were withdrawn at specific time intervals and analyzed for RFM by UV spectroscopy at $\lambda_{max}$ 475 nm. Percent drug release *vs*. time profiles were plotted. Negligible leakage of the particles from the dialysis tube was confirmed by testing the blank RFMNp, which showed no absorbance in the release medium.

*In vitro* drug-release data were fitted to kinetic models such as zero order, first order, Higuchi equation and Korsmeyer–Peppas equation. The regression analysis of $Q$ *vs*. $t$ (zero order), log $Q$ *vs*. $t$ (first order), $Q$ *vs*. square root of $t$ (Higuchi), log%$Q$ *vs*. log%$t$ (Korsmeyer–Peppas), where $Q$ is the amount of drug released at time $t$, was performed (31–33).

### Drug Loading

Measured quantity of freeze-dried nanoparticles were dissolved in methanol by sonication for 5 min and assayed for drug content on a UV spectrophotometer UV1650PC, Schimadzu Corporation US at $\lambda_{max}$ of 475 nm. Percent drug loading (DL%) was calculated using the following equation (29):

$$DL\ (\%) = W_{DL}/W_{NP} \times 100$$

where $W_{DL}$ is the weight of drug in RFMNp, and $W_{NP}$ is the weight of RFMNp.

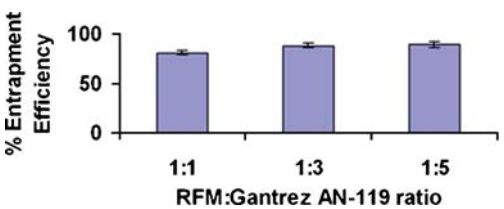


**Fig. 3.** Effect of RFM/Gantrez AN-119 ratio on entrapment efficiency of rifampicin nanoparticles at RFM/AOT molar ratio of 1:1.85

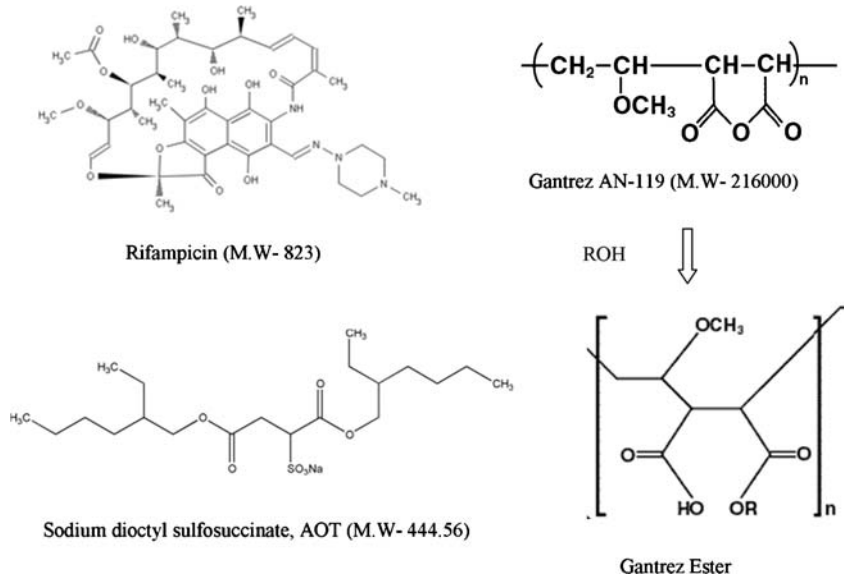


**Fig. 4.** Structures of RFM, Gantrez AN-119, AOT, and Gantrez AN-119 Ester

### Zeta Potential

Zeta potential of nanoparticle dispersion was measured using Malvern Zetasizer Nanoseries using DTS Nano software. Nanoparticle dispersion was centrifuged at 15,000 rpm for 30 min at 20°C. The resultant pellet was washed and redispersed in distilled deionized water (nanoparticles 100 µg/ml) by sonication. Samples were filled in to the folded capillary cell with the help of syringe, and the zeta potential was measured. Each sample was analyzed in triplicate.

### Transmission Electron Microscopy

The morphology/shape of nanoparticles was determined by transmission electron microscopy (TEM) on a Philips CM 200 instrument at a voltage of 200 kV having magnification of 0.23 nm using the desired magnification.

### Differential Scanning Calorimetry

Differential scanning calorimetry (DSC) thermograms of RFM, RFMNp, trehalose (cryoprotectant), AOT (surfactant), and Gantrez AN-119(polymer) were recorded on a Perkin Elmer Pyris 6 DSC (PerkinElmer, Netherlands) system in the temperature range 40–300°C at a heating rate of 10°C/min in a dynamic nitrogen atmosphere (20 ml/min). A sample of 5–6 mg was sealed in an aluminum pan, and an empty sealed aluminum pan was used as the reference.

### Powder X-ray Diffraction

Powder X-ray diffraction (PXRD) patterns for rifampicin and nanoparticles of RFM were recorded using a Rigaku Miniflex diffractometer, with Cu Kα target tube, NaI detector, variable slits, a 0.05° step size, operated at a voltage of 30 kV, 15 mA current, at 2θ/min scanning speed, and scanning angles ranged from 6° to 80° (2θ).

### Fourier Transform Infrared Spectroscopy

Infrared spectra of RFM, RFM nanoparticles, AOT, and Gantrez AN-119 were recorded on a Perkin-Elmer Fourier transform infrared (FTIR) spectrophotometer by the KBr disk method from 4,000 to 500 $cm^{-1}$.

### Stability of RFMNp

Freeze-dried nanoparticles of RFM were packed and sealed in amber glass vials and subjected to stability studies as per ICH guidelines at 30±2°C/65±5% RH and 40±2°C/75±5% RH. Samples were withdrawn at the end of 30, 60, 90, and

**Table I.** Effect of Type and Concentration of Cryoprotectant after Freeze–Thaw Study

| S. no. | Cryoprotectant | Concentration % (*w*/*v*) | Initial size (Si), nm (Avg ± std error), (*n*=3) | Final size (Sf), nm (Avg ± std error), (*n*=3) | Sf/Si ratio |
|---|---|---|---|---|---|
| 1 | Trehalose | 5 | 405.2±1.27 | 2,956.2±0.68 | 7.30 |
| | | 10 | 405.2±1.27 | 1,248.3±2.03 | 3.08 |
| | | 15 | 405.2±1.27 | 642±2.38 | 1.58 |
| | | 20 | 405.2±1.27 | 443.5±2.97 | 1.09 |
| 2 | Fructose | 5 | 405.2±1.27 | >3,000 | >7.4 |
| | | 10 | 405.2±1.27 | >3,000 | >7.4 |
| | | 15 | 405.2±1.27 | 2,431.9±0.96 | 6.00 |
| | | 20 | 405.2±1.27 | 977.9±1.48 | 2.41 |

**Table II.** Effect of Freezing Temperature and Concentration of Nanoparticles on Particle Size during Freeze–Thaw Study

| Concentration of nanoparticles (mg/ml) | Initial size (nm) | Particle size (nm) after freeze–thaw study | | | |
|---|---|---|---|---|---|
| | | Trehalose (20% *w/v*) | | Fructose (20% *w/v*) | |
| | | −40°C | −70°C | −40°C | −70°C |
| 8 | 382.5±2.01 | 386.9±2.24 | 394.6±2.31 | 746.1±3.13 | 774±3.52 |
| 16 | 373.5±2.45 | 403.6±2.81 | 389.4±3.11 | 758.3±2.76 | 737.6±2.63 |
| 32 | 405.2±1.27 | 443.5±1.75 | 436.5±3.28 | 977.9±1.89 | 861.2±2.28 |
| 64 | 411.6±1.96 | 971.5±2.59 | 991.5±1.86 | 1,203.5±1.67 | 1,289.5±2.05 |

180 days and evaluated for *in vitro* drug release, redispersibility of nanoparticles, particle size, and drug content.

## RESULTS AND DISCUSSION

### Nanoparticles of RFM

RFM Gantrez nanoparticles prepared without AOT revealed low entrapment efficiency (EE) (less than 15%). Inclusion of AOT resulted in significant increase in EE due to ionic interaction between positive charge on RFM and anionic AOT. Formation of nanoparticles was observed only when all the three components, i.e., RFM, AOT, and Gantez AN-119 are present together. Increase in AOT concentration resulted in increase EE upto a molar ratio of 1:1.85. Further increase in molar ratio of RFM/AOT did not result in increase in EE (Fig. 2), whereas there was no effect on EE with change in the RFM/Gantrez AN-119 ratios at RFM/AOT molar ratio of 1:1.85 (Fig. 3), suggesting the role of AOT in complex formation. The negative charge on $-SO_3^-$ (succinate) group of AOT reacts with positive charge on 3-piperazine nitrogen group of RFM to form an ionic complex. With both RFM and AOT being small molecules, the reaction could take place in stoichiometric ratios exhibiting maximum interaction at RFM/AOT molar ratio of 1:1.85 (EE 90±2.5%). Although Gantrez AN-119 has number of negative charges, it is possible that they are partially converted to $-COOC_2H_5$ group in presence of ethanol (Fig. 4). Moreover, with Gantrez AN-119 (mol wt.216,000) being of high molecular weight, steric hindrance could have prevented interaction of negatively charged groups of Gantrez AN-119 with positively charged RFM.

Further, better nanoparticle stability has been reported using anionic surfactant sodium deoxycholate as compared to non-ionic surfactant Pluronic PE F68 (23); hence, anionic AOT could provide better stability to nanoparticle dispersion due to electrostatic repulsion. PVA was used as stabilizer (26,34,35). Particle size of nanoparticles ranged between 375 and 490 nm (Fig. 2), which is considered suitable for macrophage uptake (28,36).

### Freeze–Thaw Study

The physicochemical properties of nanoparticles have an effect on their efficiency in drug delivery (14). If particles are stored as a suspension in an aqueous medium, degradation and/or solubilization of the polymer, drug leakage, drug desorption, and/or drug degradation may occur. Lyophilization represents one of the most useful methodology to ensure the long-term conservation of unloaded or drug-bound polymeric nanoparticles (25,34,35,37). After freeze drying, easy and rapid reconstitution and unchanged particle size of the product are important features. Freeze thaw represent a quick and economical method to assess effect of cryoprotectant on particle aggregation.

Carbohydrates are favored as freeze-drying excipients since they are chemically innocuous and can be easily vitrified during freezing (14). Carbohydrates as cryoprotectant have proved to be superior to polyalcohols. Hence, the two carbohydrates, a disaccharide trehalose and a monosaccharide fructose, were selected for the study (18,23,27).

Samples with cryoprotectants showed concentration-dependent cryoprotection and revealed greater increase in particle size at lower cryoprotectant concentrations (38). Large aggregates were clearly observed in samples frozen without cryoprotectant, and hence, their particle size was not determined. At equivalent concentration, trehalose proved to be a better cryoprotectant than fructose (Table I). Trehalose

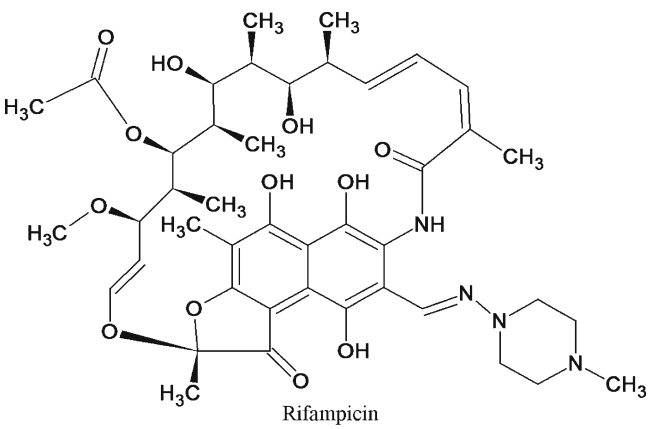


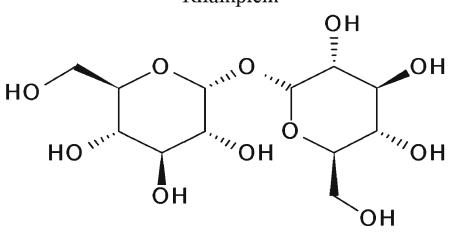


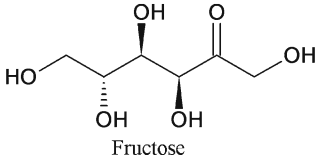


**Fig. 5.** Structures of rifampicin, trehalose, and fructose

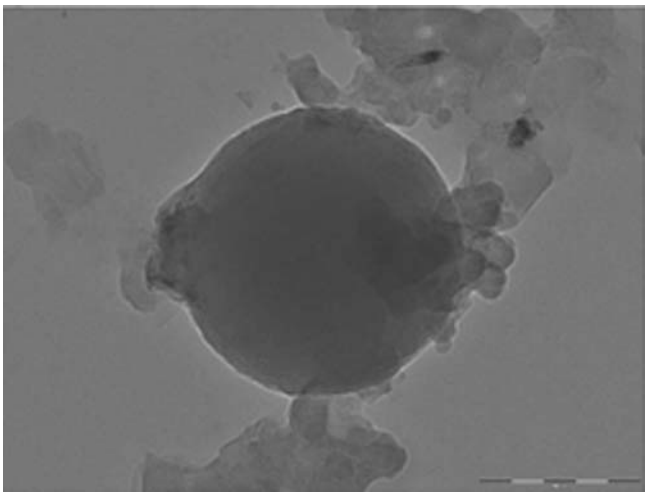

**Fig. 6.** Transmission electron microscopic image of rifampicin nanoparticle

at 20% *w*/*v* revealed minimal increase in particle size with a Sf/Si ratio (Sf—final size, Si—initial size) of 1.09, which being less than 1.3 is considered acceptable (12), while fructose at the same concentration revealed a high Sf/Si ratio of 2.41 after the freeze–thaw study. At lower concentrations of trehalose and fructose, Sf/Si ratios were correspondingly higher (Table I).

Fructose as cryoprotectant revealed an increase in particle size with increase in nanoparticle concentration in the dispersion. Trehalose however revealed no significant difference in particle size up to a concentration of 32 mg/ml, while above this concentration, there was a significant increase in particle size. This suggested trehalose as a more suitable cryoprotectant. Similar behavior was observed at both the freezing temperatures (Table II).

When the nanoparticle dispersion containing cryoprotectant is frozen below glass transition temperature, the cryoprotectants form a glassy/vitreous coating around the nanoparticles protecting them against stresses like mechanical stress of ice crystals, thereby preventing aggregation. Insufficient concentration of cryoprotectant leads to incomplete coating of glassy matrix around nanoparticles favoring aggregation. Further, according to the particle isolation hypothesis, the spatial separation of particles within the unfrozen fraction results in insufficient cryoprotectant at higher concentration of nanoparticles, leading to aggregation. Particle isolation hypothesis suggest that the separation of individual particles within the unfrozen fraction prevents aggregation during freezing. According to this hypothesis, sufficient quantities of virtually any excipient should offer similar protection during freezing. Furthermore, the concentrated suspensions employed in clinical trials may be difficult to preserve by lyophilization (36). Freezing temperature below $T_g'$ of cryoprotectant has no effect on the glassy protective matrix of cryoprotectant formed around the nanoparticles. Freeze–thaw study was carried out at temperatures below the $T_g'$ of cryoprotectants used (27), and hence, it is expected to have no effect on stability, aggregation, and redispersion properties of freeze-dried nanoparticle preparation. It has been reported that there was a negligible increase in Sf/Si ratio of poly(D,L-lactic acid) nanoparticles during freeze thawing at two different temperatures, i.e., −55°C and at −196°C with trehalose (26).

Trehalose showed better cryoprotectant effect than fructose because trehalose is a non-reducing sugar and exists only in closed ring form. Absence of internal hydrogen bonds in trehalose allows more flexible formation of hydrogen bonds between its –OH groups and free carboxylic group of Gantrez AN-119 on nanoparticles during freeze drying. Gantrez AN-119 is an anhydride which opens up to carboxylic group, which could interact and form hydrogen bonds with –OH groups of trehalose. Fructose is a reducing sugar and can exist both in chain and ring form. Hence it forms internal hydrogen bonds, and less groups are available to form hydrogen bonds with nanoparticle surfaces (7,26,28). It has been reported that the cryoprotective effect was related to the hydrogen bonding capability of the sugars used as cryoprotectants (26). Moreover, trehalose has one of the highest glass transition temperatures ($T_g$) of all saccharides commonly used (TREHA™, trehalose by Hayashibara, Japan), and disaccharides like trehalose appear to have a greater influence on the vitrification properties or they are more active than monosaccharides like fructose. The lower the $T_g$, the more the lyophilizates tend to collapse. Trehalose is very often considered as the best cryoprotective agent among the available carbohydrates (7,23,27). Our study

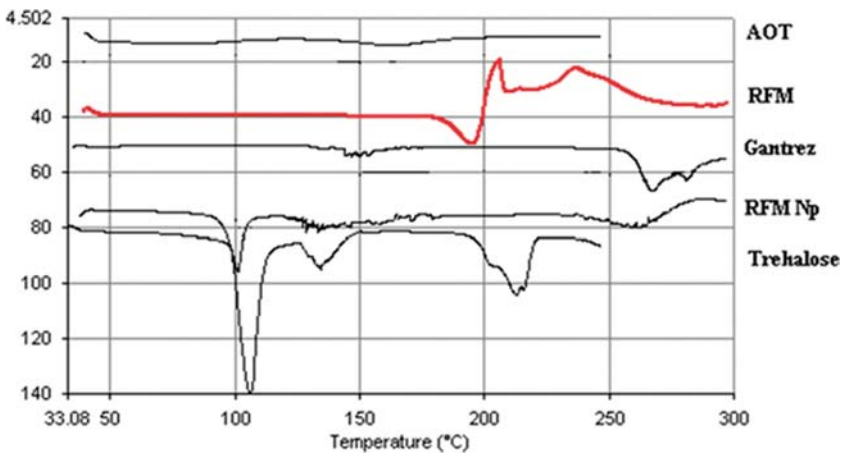


**Fig. 7.** DSC thermograms of RFM, rifampicin nanoparticles, and excipients

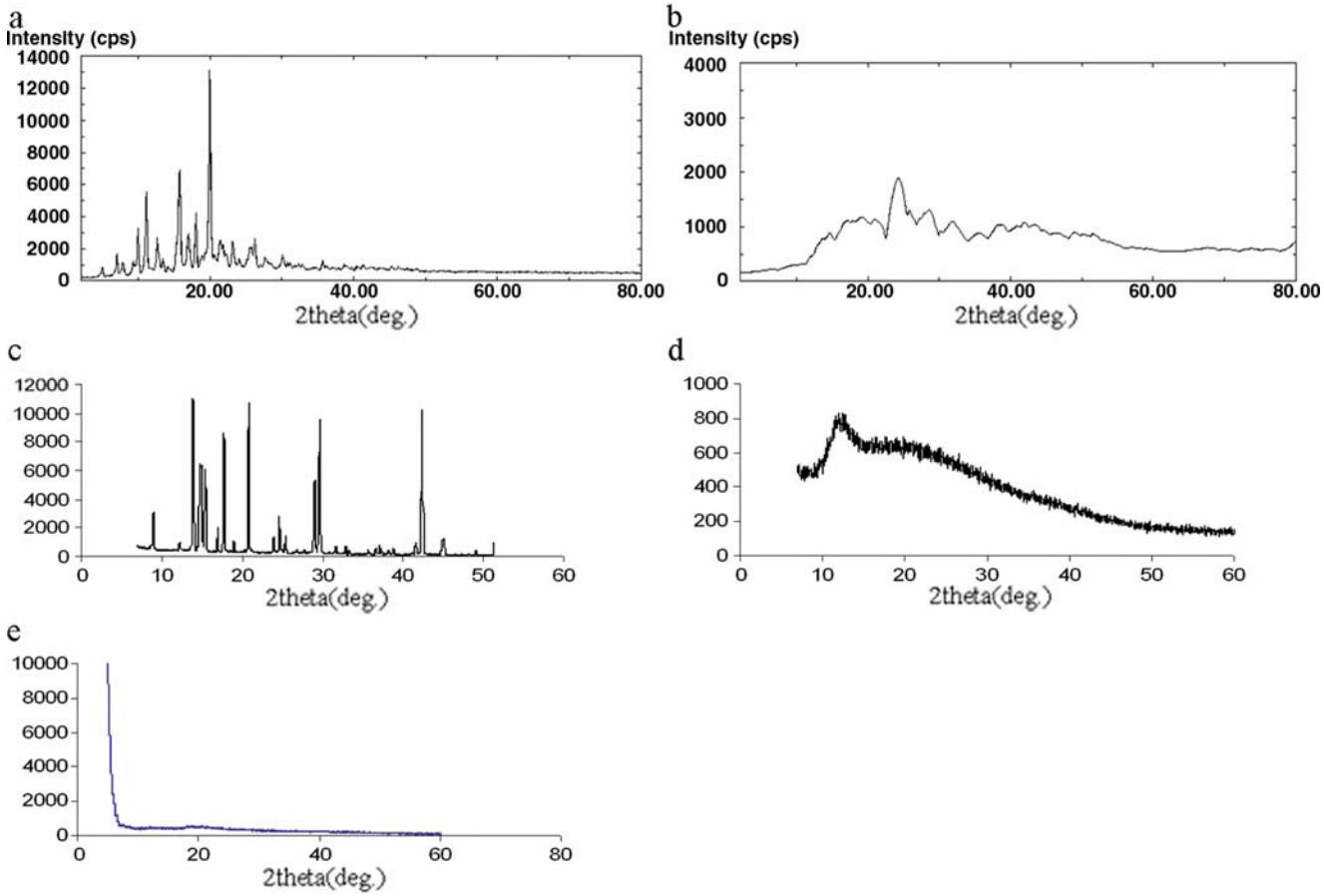


**Fig. 8.** **a** X-ray powder diffractograms of RFM, **b** X-ray powder diffractograms of rifampicin nanoparticles, **c** X-ray powder diffractograms of trehalose, **d** X-ray powder diffractograms of Gantrez AN-119, **e** X-ray diffractograms of AOT

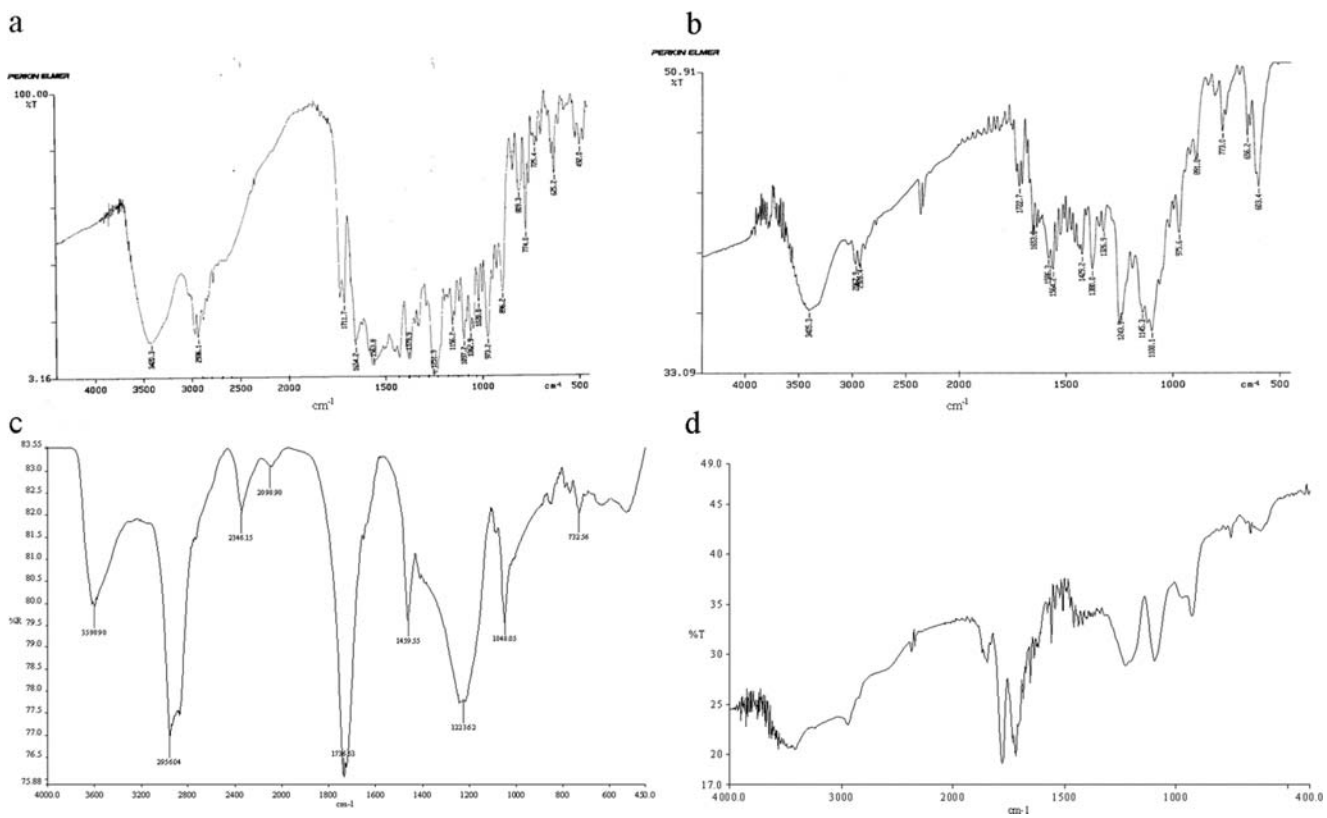


**Fig. 9.** **a** FTIR spectrum of RFM, **b** FTIR spectrum of rifampicin nanoparticles, **c** FTIR spectrum of AOT, **d** FTIR spectrum of Gantrez AN-119

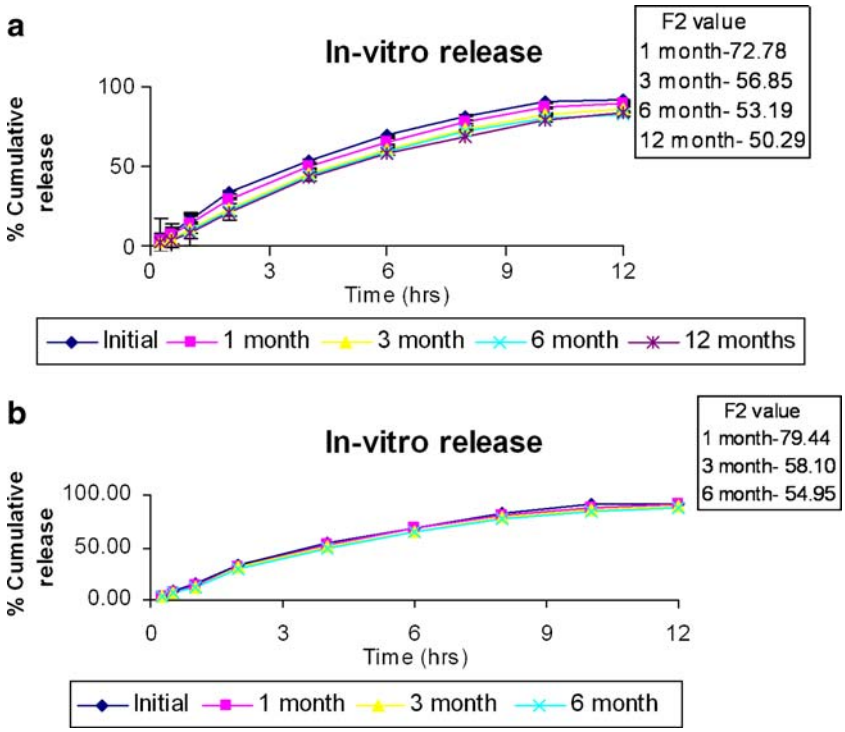


**Fig. 10.** **a** *In vitro* release and stability of rifampicin nanoparticles at 30±2°C/65±5% RH. **b** *In vitro* release and stability of rifampicin nanoparticles at 40±2°C/75±5% RH

supports this observation. The structures of rifampicin and the two cryoprotectants, i.e., trehalose and fructose, have been shown in Fig. 5.

### Freeze Drying of RFMNp

To determine the correlation between the freeze–thaw study and freeze drying, samples containing trehalose and fructose at 20% *w/v* were freeze-dried. Freeze-dried nanoparticles with trehalose and fructose (20% *w/v*) as cryoprotectants revealed similar behavior in particle size as that observed during the freeze–thaw study. Trehalose showed marginal increase in particle size with a Sf/Si ratio of 1.10 while fructose revealed significant increase in particle size with a Sf/Si ratio of 2.52.

Freeze–thaw study correlated well with freeze drying and can be used as a pre-test for screening of type and concentration of cryoprotectants used in freeze drying. Similar correlation has been reported by others (7,12,18,23).

### Freeze-dried RFMNp

Freeze-dried nanoparticles revealed drug loading of 13.04% and zeta potential of −34.52 mV. A zeta potential of ±30 mV dictates generally sufficient colloidal stability of nanoparticles (39). TEM image of RFMNp is shown in Fig. 6. The average diameter of RFMNp was 400±25 nm by PCS. The results of particle size by PCS and TEM are comparable. TEM revealed spherical particles.

**Table III.** *In Vitro* Release Data of RFMNp—Model Fitting

| Model | $r^2$ | Slope | Intercept |
|---|---|---|---|
| Zero order | 0.95188 | 7.87775 | 16.9272 |
| First order | −0.9953 | −0.0966 | 2.00372 |
| Higuchi | 0.98186 | 32.626 | −8.3105 |
| Korsmeyer–Peppas | 0.9788 | 0.8245 (*n*) | 1.1833 |

### Differential Scanning Calorimetry

DSC enables detection of all the processes in which energy is required or produced (i.e., endothermic and exothermic phase transformations). The thermograms of RFM, RFMNp, trehalose, Gantrez AN-119, and AOT are shown in Fig. 7. Pure RFM revealed a melting endotherm between 180°C and 200°C corresponding to melting point of the drug indicating crystalline nature. The disappearance of RFM melting endotherm in RFMNp suggests its amorphous form.

### Powder X-ray Diffraction

Crystallinity in the sample is reflected by a characteristic fingerprint region in the diffraction pattern. The XRD spectra

**Table IV.** Stability Data of RFMNp

| | 30°C/65% RH | | 40°C/75% RH | |
|---|---|---|---|---|
| RFM | Drug content % | Sf/Si ratio | Drug content % | Sf/Si ratio |
| Initial | 100% | | 100% | |
| 1 month | 96.9±0.19 | 1.01 | 99.5±0.37 | 1.01 |
| 3 month | 92.1±0.81 | 1.08 | 93.44±0.65 | 1.09 |
| 6 month | 92.8±0.054 | 1.16 | 91.81±0.95 | 1.15 |
| 12 months | 90.11±0.74 | 1.165 | | |

of RFM, RFMNp, trehalose, Gantrez AN-119, and AOT are shown in Fig. 8. RFM and trehalose are highly crystalline powders showing characteristic sharp diffraction peaks. These sharp diffraction peaks disappeared in the RFMNp, indicating amorphization of the drug.

### Fourier Transform Infrared Spectroscopy

The Fourier transform infrared spectrum of RFM, RFMNp, Gantrez AN-119, and AOT are shown in Fig. 9. The presences of characteristic peaks associated with specific structural characteristics of the drug molecule are observed both in RFM and nanoparticles of RFM (Fig. 9a, b), respectively. The absorption band of O–H and N–H stretching vibration of RFM around 3,420.3 $cm^{-1}$, C–H stretching at 2,936 $cm^{-1}$, –C=O acetyl stretching at1,730, and 1,711.7, –C=N– asymmetric stretching at 1,654.2 $cm^{-1}$, C=C stretching at 1,563 $cm^{-1}$, C–N stretching at 1,379.9 $cm^{-1}$, and –C–O–C– ether group at 1,251.9 were observed in RFM drug. In case of RFMNp also the major peaks associated with RFM were observed, such as O–H and N–H stretching vibration of RFM around 3,405.3 $cm^{-1}$, C–H stretching at 2,967.9 $cm^{-1}$, C=O acetyl stretching at1,722.7 $cm^{-1}$, –C=N- asymmetric stretching at 1,653.8 $cm^{-1}$, C=C stretching at 1,564.2 $cm^{-1}$, C–N stretching at 1,380 $cm^{-1}$, and –C–O–C– ether group at 1,243.9. Thus there seems to be no chemical interaction between drug and carrier. A chemical interaction could occur between 3-piperazine nitrogen having p$K_a$ 7.9 and the succinate group of AOT. This explains the high entrapment efficiency of RFM in nanoparticles in presence of AOT. This interaction is not visualized in IR due to overlap with NH group of RFM at the eighth position. Further, large numbers of groups are present, which tend to have masking effect on IR peaks, which are otherwise visible.

### *In vitro* Drug Release

Nanoparticles showed sustained release of RFM up to 24 h, which may be due to slow release of drug from the complex (Fig. 10a). It is possible that phosphate ions of the dissolution medium complex with AOT to allow release of RFM, which is then released from the nanoparticles by diffusion.

To investigate the drug-release kinetics, data were fitted to various kinetic models such as zero order, first order, Higuchi equation, and Korsmeyer–Peppas equation. The results of curve fitting of RFMNp into different mathematical models are given in Table III. The plots of percent cumulative drug release *vs*. square root of time were found to be linear with higher correlation coefficient value ($r^2$=0.98186), and following the Higuchi square root model, the mechanism of drug release from the nanoparticles is suggested as diffusion controlled (31–33). Hence ion exchange followed by diffusion is suggested as the mechanism of drug release.

### Stability and Redispersibility of RFMNp

Freeze-dried nanoparticles were stable as per ICH guidelines at 30±2°C/65±5% RH and 40±2°C/75±5% RH and revealed good redispersibility, and there was no significant change in particle size as indicated by Sf/Si ratio <1.3, drug content (Table IV), and *in vitro* release as indicated by F2 value (Fig. 10a, b).

## CONCLUSION

The results of the freeze–thaw study correlated well with actual freeze-dried samples. Freeze–thaw study therefore represents a simple and predictable approach in the selection of cryoprotectants for freeze drying and can be used as a pretest for screening of type and concentration of cryoprotectants used in freeze drying. This simple approach could prove to be cost efficient and time saving.

## ACKNOWLEDGMENTS

The authors wish to acknowledge the Department of Biotechnology (DBT), Government of India, for the grant, and senior research fellowship to Praveen Date, and IIT-B, Mumbai for the TEM study.

## REFERENCES

1. Kreuter J. Nanoparticles and microparticles for drug and vaccine delivery. J Anat. 1996;189:503–5.
2. McClean S, Prosser E, Meehan E, O'Malley D, Clarke N, Ramtoola Z, *et al*. Binding and uptake of biodegradable polydl-lactide micro- and nanoparticles in intestinal epithelia. Eur J Pharm Sci. 1998;6:153–63.
3. Rodriguez GS, Allémann E, Fessi H, Doelker E. Physicochemical parameters associated with nanoparticle formation in the salting-out, emulsification-diffusion, and nanoprecipitation methods. Pharm Res. 2004;21:1428–39.
4. Oppenheim R. Solid colloidal drug delivery systems: nanoparticles. Int J Pharm. 1981;8:217–34.
5. Alonso MJ. Nanoparticulate drug carrier technology. In: Cohen S, Bernstein H, editors. Microparticulate systems for the delivery of proteins and vaccines. New York: Marcel Dekker; 1996. p. 203–42. Book chapter.
6. Brigger I, Dubernet C, Couvreur P. Nanoparticles in cancer therapy and diagnosis. Adv Drug Deliv Rev. 2002;54:631–51.
7. Abdelwahed W, Degobert G, Stainmesse S, Fessi H. Freeze-drying of nanoparticles: formulation, process and storage considerations. Adv Drug Deliv Rev. 2006;58:1688–713.
8. Storm G, Belliot SO, Daemen T, Lasic D. Surface modification of nanoparticles to oppose uptake by the mononuclear phagocyte system. Adv Drug Deliv Rev. 1995;17:31–48.
9. Panyam J, Labhasetwar V. Biodegradable nanoparticles for drug and gene delivery to cells and tissue. Adv Drug Deliv Rev. 2003;55:329–47.
10. Desai MP, Labhasetwar V, Walter E, Levy RJ, Amidon GL. The mechanism of uptake of biodegradable microparticles in Caco-2 cells is size dependent. Pharm Res. 1997;14:1568–73.
11. Jaeghere DF, Allemann E, Leroux JC, Stevels W, Feijen J, Doelker E, *et al*. Formulation and lyoprotection of poly (lactic acid-co-ethylene oxide) nanoparticles: influence on physical stability and *in vitro* cell uptake. Pharm Res. 1999;16:859–66.
12. Saez A, Guzma'n M, Molpeceres J, Aberturas MR. Freeze drying of polycaprolactone and poly(D, L-lactic-glycolic) nanoparticles induce minor particle size changes affecting the oral pharmacokinetics of loaded drugs. Eur J Pharm Biopharm. 2000;50:379–87.
13. Chacon M, Molpeceres J, Berges L, Guzman M, Aberturas MR. Stability and freeze-drying of cyclosporine loaded poly(D, L lactide-glycolide) carriers. Eur J Pharm Sci. 1999;8:99–107.
14. Bozdag S, Dillen K, Vandervoort J, Ludwig A. The effect of freeze-drying with different cryoprotectants and gamma-irradiation sterilization on the characteristics of ciprofloxacin HCl-loaded

poly(D, L-lactide-glycolide) nanoparticles. J Pharm Pharmacol. 2005;57:699–707.
15. Crowe LM, Reid DS, Crowe JH. Is trehalose special for preserving dry materials? Biophys J. 1996;71:2087–93.
16. Engel A, Bendas G, Wilhelm F, Mannova M, Ausborn M, Nuhn P. Freeze-drying of liposomes with free and membrane-bound cryoprotectives-the background of protection and damaging process. Int J Pharm. 1994;107:99–110.
17. Tanaka K, Takeda T, Fuji K, Miyajima K. Cryoprotective mechanism of saccharides on freeze-drying of liposome. Chem Pharm Bull. 1992;40:1–5.
18. Schwarz C, Mehnert W. Freeze-drying of drug-free and drug-loaded solid lipid nanoparticles (SLN). Int J Pharm. 1997;157:171–9.
19. Shahgaldian P, Gualbert J, Aıssa K, Coleman AW. A study of the freeze-drying conditions of calixarene based solid lipid nanoparticles. Eur J Pharm Biopharm. 2003;55:181–4.
20. Cavalli R, Caputo O, Carlotti ME, Trotta M, Scarnecchia C, Gasco MR. Sterilization and freeze-drying of drug-free and drug-loaded solid lipid nanoparticles. Int J Pharm. 1997;148: 47–54.
21. Zhang L, Liu L, Qian Y, Chen Y. The effects of cryoprotectants on the freeze-drying of ibuprofen-loaded solid lipid microparticles (SLM). Eur J Pharm Biopharm. 2008;69:750–9.
22. Talsma H, Steenbergen MJV, Salemink PJM, Crommelin DJA. The cryopreservation of liposomes: a differential scanning calorimetry study of the thermal behavior of a liposome dispersion containing mannitol during freezing/thawing. Pharm Res. 1991;8:1021–6.
23. Chasteigner SD, Cave G, Fessi H, Devissaguet JP, Puisieux F. Freeze-drying of itraconazole-loaded nanosphere suspensions: a feasibility study. Drug Dev Res. 1996;38:116–24.
24. Kristl J, AlleÂmann E, Gurny R. Formulation and evaluation of zinc phthalocyanine-loaded poly(dl-lactic acid) nanoparticles. Acta Pharm. 1996;46:1–12.
25. Roy D, Guillon X, Lescure F, Couvreur P, Bru P, Breton P. On shelf stability of freeze-dried poly(methylidene malonate, 2.1.2) nanoparticles. Int J Pharm. 1997;148:165–75.
26. Guerrero DQ, Quintanar GA, AlleÂmann E, Fessi H, Doelker E. Influence of the stabilizer coating layer on the purification and freeze-drying of poly(d, l-lactic acid) nanoparticles prepared by an emulsion-diffusion technique. J Microencapsul. 1998;15:107–19.
27. Franks F. Freeze-drying of bioproducts: putting principles into practice. Eur J Pharm Biopharm. 1998;45:221–9.
28. Abdelwahed W, Degobert G, Fessi H. Investigation of nanocapsules stabilization by amorphous excipients during freeze-drying and storage. Eur J Pharm Biopharm. 2006;63:87–94.
29. Li Y, Wong HL, Shuhendler AJ, Rauth AM, Wu XY. Molecular interactions, internal structure and drug release kinetics of rationally developed polymer–lipid hybrid nanoparticles. J Control Release. 2008;128:60–70.
30. Muttil P, Kaur J, Kumar K, Yadav AB, Sharma R, Misra A. Inhalable microparticles containing large payload of anti-tuberculosis drugs. Eur J Pharm Sci. 2007;32:140–50.
31. Thakkar VT, Shah PA, Soni TG, Parmar MY, Gohel MC, Gandhi TR. Goodness-of-fit model-dependent approach for release kinetics of levofloxacin hemihydrates floating tablet. Dissolution Technologies. 2009;16:35–9.
32. Shivakumar HN, Patel PB, Desai BG, Purnima A, Arulmozhi S. Design and statistical optimization of glipizide loaded lipospheres using response surface methodology. Acta Pharm. 2007;57:269–85.
33. Shoaib MH, Tazeen J, Merchant HA, Yousuf RI. Evaluation of drug release kinetics from ibuprofen matrix tablets using HPMC. Pak J Pharm Sci. 2006;19:119–24.
34. Abdelwahed W, Degobert G, Fessi H. A pilot study of freeze drying of poly(epsiloncaprolactone) nanocapsules stabilized by poly(vinyl alcohol): formulation and process optimization. Int J Pharm. 2006;17:178–88.
35. Abdelwahed W, Degobert G, Fessi H. Freeze-drying of nanocapsules: impact of annealing on the drying process. Int J Pharm. 2006;324:74–82.
36. Allison SD, Molina MDC, Anchordoquy TJ. Stabilization of lipid/DNA complexes during the freezing step of the lyophilization process: the particle isolation hypothesis. Biochim Biophys Acta. 2000;1468:127–38.
37. Kuleshova LL, MacFarlane DR, Trounson AO, Shaw JM. Sugars exert a major influence on the vitrification properties of ethylene glycol-based solutions and have low toxicity to embryos and oocytes. Cryobiology. 1999;38:119–30.
38. Sugrue S. Predicting and controlling colloid suspension stability using electrophoretic mobility and particle size measurements. Am Lab. 1992;24:64–71.
39. Ahsan F, Rivas IP, Khan MA, Suarez AIT. Targeting to macrophages: role of physicochemical properties of particulate carriers—liposomes and microspheres—on the phagocytosis by macrophages. J Control Release. 2002;79:29–40.